ELSEVIER

Contents lists available at ScienceDirect

Process Safety and Environmental Protection

ChemE ADVANCING CHEMICAL BY SIGNERING BY MACHERINGS

journal homepage: www.elsevier.com/locate/psep

Investigation of the removal and recovery of nitrate by an amine-enriched composite under different fixed-bed column conditions



Ali Ansari, Enrico Tapire Nadres, Minh Đồ, Debora Frigi Rodrigues*

Department of Civil and Environmental Engineering, Room N136 Engineering Building 1, University of Houston, TX, 77204-4003, USA

ARTICLE INFO

Article history: Received 16 December 2020 Received in revised form 14 April 2021 Accepted 20 April 2021 Available online 24 April 2021

Keywords:
Nitrate
Chitosan
Polyethyleneimine
Continuous adsorption
Breakthrough models

ABSTRACT

Continuous adsorption of nitrate in a fixed-bed column can be an effective method for its removal from water. In this study, an amine-rich polymer composite adsorbent was prepared by crosslinking chitosan (CS) and polyethyleneimine (PEI) with glutaraldehyde (GLA). The CS-PEI-GLA was packed into columns and the effect of flow rate, influent concentration, bed height, and other ionic species on the column performance was investigated. The highest adsorption capacity was achieved at the lowest flow rate and highest influent concentration and bed height. Maximum adsorption capacity of 137.62 mg NO₃⁻-N/g was determined from the Thomas model. The column had acceptable nitrate removal in the presence of 1000 ppm chloride but poor performance in the presence of 1000 ppm sulfate due to the competitive effect of sulfate for binding sites. The best recovery agent was 0.5 M NaCl as it could regenerate the column to <90 % of its capacity after 10 adsorption-desorption cycles. The adsorbent effectively removed nitrate as well as phosphate and total organic carbon from a real water sample. This study suggests that amine rich polymers can be good candidates for the removal of nitrate in contaminated water.

 $\hbox{@ 2021}$ Institution of Chemical Engineers. Published by Elsevier B.V. All rights reserved.

1. Introduction

Nitrate (NO₃⁻) contamination in surface and groundwater can be originated from different sources like agricultural runoff, domestic wastewater, and effluent of industries producing fertilizers, pharmaceuticals, food, and explosives (Salman Tabrizi and Yavari, 2020; Jóźwiak et al., 2014; Xing et al., 2011). This contamination can cause different problems, for instance, disruption of conventional wastewater treatment plant, eutrophication, harmful effect on aquatic life, and adverse effects on human health like respiratory tract infection, hypertension, cyanosis syndrome, and blue-baby syndrome in infants (Salman Tabrizi and Yavari, 2020; Jóźwiak et al., 2014; Xing et al., 2011; Najmi et al., 2020; Xu et al., 2013; Nur et al., 2015). Moreover, nitrate can cause gastrointestinal tract cancer and transform into other carcinogenic compounds, like nitrite and nitrosamines (Jóźwiak et al., 2014; Najmi et al., 2020; Wu et al., 2016; Olgun et al., 2013). Because of these risks associated with nitrate, according to World Health Organization (WHO), its concentration in drinking water should not be higher than 45 mg/L NO₃or 10 mg/L NO₃ -- N (Xu et al., 2013). The high solubility and stability

of nitrate in water have made its removal challenging using conventional methods (Salman Tabrizi and Yavari, 2020). As of today, different methods are suggested for nitrate removal, such as reverse osmosis, electrodialysis, biological and chemical denitrification, ion exchange, and adsorption. The latter has attracted a lot of attention because it is fast, simple, cheap, and flexible (Salman Tabrizi and Yavari, 2020; Najmi et al., 2020; Wu et al., 2016). Furthermore, adsorbents can be reused, as a result, the amount of sludge for disposal are not high (Xu et al., 2013; Olgun et al., 2013).

The heart of an adsorption process is the type of adsorbent that is chosen to adsorb the pollutant. Since nitrate is an anion, it is expected that an adsorbent with positively charged functional groups would show a promising performance for nitrate removal (Salman Tabrizi and Yavari, 2020). Therefore, amine functional groups, which are protonated at pH below 9 were hypothesized to be good candidates for nitrate adsorption (Salman Tabrizi and Yavari, 2020; Rao et al., 2019). Chitosan (CS) and polyethyleneimine (PEI) are both amine-rich polymers, thus they could potentially be used as effective adsorbents for nitrate removal (Salman Tabrizi and Yavari, 2020; Golie and Upadhyayula, 2016; Sun and Zheng, 2020; Berbar et al., 2012; Nadres et al., 2017a). Chitosan is a renewable source, since it is a waste product from the crab and shrimp canning industries, and can be obtained on an industrial scale (Dutta et al., 2004). In its chemical structure, abundant amine and hydroxyl

^{*} Corresponding author. E-mail address: dfrigirodrigues@uh.edu (D.F. Rodrigues).

Nomenclature

a Logistic function parameterB Logistic function parameter (1/min)

BDST Bed depth service time

C₀ Nitrate-N concentration in influent (mg/L)

C_b Nitrate-N concentration at breakthrough point

(mg/L)

C_e Nitrate-N concentration in effluent (mg/L)

CS Chitosan

CWS Community water service

GLA Glutaraldehyde H Bed height (cm) ISE Ion-selective electrode

K_{B-A} Bohart-Adams rate constant (L/mg.min)
 K_{BDST} BDST model rate constant (L/mg.min)
 KHP Potassium hydrogen phthalate
 K_{Th} Thomas rate constant (L/mg.min)
 K_{Y-N} Yoon-Nelson rate constant (1/min)

M Adsorbent mass (g) MTZ Mass-transfer zone

 $\begin{array}{ll} N_{BDST} & BDST \ model \ volumetric \ adsorption \ capacity \ (mg/L) \\ N_m & Bohart-Adams \ adsorption \ capacity \ per \ unit \ volume \end{array}$

(mg/L)

PEI Polyethyleneimine Q Flow rate (L/min)

q_{exp} Experimental adsorption capacity (mg/g) q_m Thomas adsorption capacity (mg/g)

R Percent removal
R² Regression coefficient

t Time (min)

t_b Time at the breakthrough point (min)

u Linear velocity (cm/min)

V_b Total effluent volume up to the breakthrough point

(mL)

WHO World Health Organization

τ Time when adsorbate reaches to half of break-

through (min)

functional groups exist. These functional groups can effectively remove different aquatic pollutants (Golie and Upadhyayula, 2016; Crini and Badot, 2008; Medina et al., 2016; Perez et al., 2017). However, both CS and PEI are unstable, therefore chemical enhancement is necessary to make them suitable for adsorption (Salman Tabrizi and Yavari, 2020; Jóźwiak et al., 2014; Golie and Upadhyayula, 2016; Nadres et al., 2017b). In our previous study (Nadres et al., 2017a), a novel polymer composite was prepared by cross-linking CS and PEI using glutaraldehyde (GLA). The CS-PEI-GLA adsorbent showed good stability and nitrate removal performance over a wide range of pHs in batch mode (Nadres et al., 2017a). However, in terms of practicality, an adsorbent should be evaluated in continuous mode. Although the batch experiments provided information about some characteristics of the adsorbent, since the continuous adsorption does not necessarily reach equilibrium like the batch adsorption, testing the adsorbent performance in continuous mode is essential (Salman Tabrizi and Yavari, 2020; Najmi et al., 2020). Furthermore, the effect of hydrodynamic parameters, like flow rate cannot be assessed in the batch mode, as a result, designing an effective industrial-scale continuous adsorption system must be based on the data obtained from a lab-scale continuous column (Salman Tabrizi and Yavari, 2020; Najmi et al., 2020; Golie and Upadhyayula, 2016).

In this study, a fixed-bed column packed with the CS-PEI-GLA was used to remove nitrate from the aqueous phase continuously.

Breakthrough curves were obtained for the column under different flow rates, influent concentrations, and bed heights. Logistic function parameters were obtained by fitting the experimental data and these parameters were used to calculate the Bohart-Adams, Thomas, and Yoon-Nelson models' parameters. The breakthrough curves and models' parameters are essential for industrial-scale column design. Effect of coexisting anions namely sulfate and chloride, on nitrate adsorption was also investigated. Finally, regeneration and reusability of the column, as well as nitrate removal from a real water sample were determined.

2. Material and methods

2.1. Synthesis and characterization of the adsorbent (CS-PEI-GLA)

The description of materials used in this study is provided in the supporting information. Adsorbent synthesis, optimization, and characterization procedures have been reported in our previous publication (Nadres et al., 2017a). Briefly, a solution containing 2% w/w CS and 10 % w/w PEI was prepared and stirred for 16 h. Followed by addition of GLA at a final concentration of 2% w/w. After GLA addition, the solution turned into a gel. The gel was further washed and freeze-dried to obtain a brownish powder (CS-PEI-GLA). The prepared adsorbent was characterized by Attenuated Total Reflectance Fourier Transform Infrared spectroscopy (ATR-FTIR), X-ray photoelectron spectroscopy (XPS), Brunauer-Emmett-Teller (BET), and Scanning Electron Microscopy (SEM) as described by (Nadres et al., 2017a).

2.2. Nitrate adsorption optimization: column experiments

A weighed amount of dried CS-PEI-GLA adsorbent was swelled overnight in deionized water. The column was prepared by packing the adsorbent into a glass column (15 mm, inner diameter and 30 cm height) and washed with five volumes of deionized water. The influent at pH = 7 was introduced to the column from a three liters Erlenmeyer flask using a peristaltic pump. The effluent was collected using a fraction collector (Fig. 1).

It was investigated how breakthrough curves as well as the parameters described below are affected by changes in rate of flow, nitrate concentration in the influent, and the height of the bed.

(a) experimental adsorption capacity q_{exp} (mg/g),

$$q_{exp} = \frac{QC_0 \int_{t=0}^{t=total} (1 - \frac{C_e}{C_0}) dt}{M}$$
 (1)

where C_0 and C_e (mg/L) are the nitrate-N concentration in influent and effluent, respectively, t (min) is the time, Q (L/min) is the flow rate, and M (g) is the adsorbent mass,

(b) nitrate removal R (%),

$$R = \frac{q_{exp}}{QC_0t_e} \tag{2}$$

where t_e (min) is exhaustion time, when the C_e equals 0.95 of C_0 , (c) total effluent volume up to the breakthrough point, C_e equals $10 \text{ mg/L NO}_3^-\text{-N}$, V_h (mL),

$$V_b = Qt_b \tag{3}$$

where t_b is the time at the breakthrough point.

The flow rate of the pump was varied (5, 7.5, 10 mL/min), while using a constant amount of adsorbent (0.5 g) and nitrate concentration $(100 \text{ mg/L NO}_3^-\text{-N})$, to investigate the correlation between flow rate and nitrate adsorption. Different concentrations of the influent $(50, 100, 200 \text{ mg/mL NO}_3^-\text{-N})$, while using constant flow rate (5 mL/min) and amount of adsorbent (0.5 g), were used to determine their effect on the efficiency of nitrate removal. Finally,

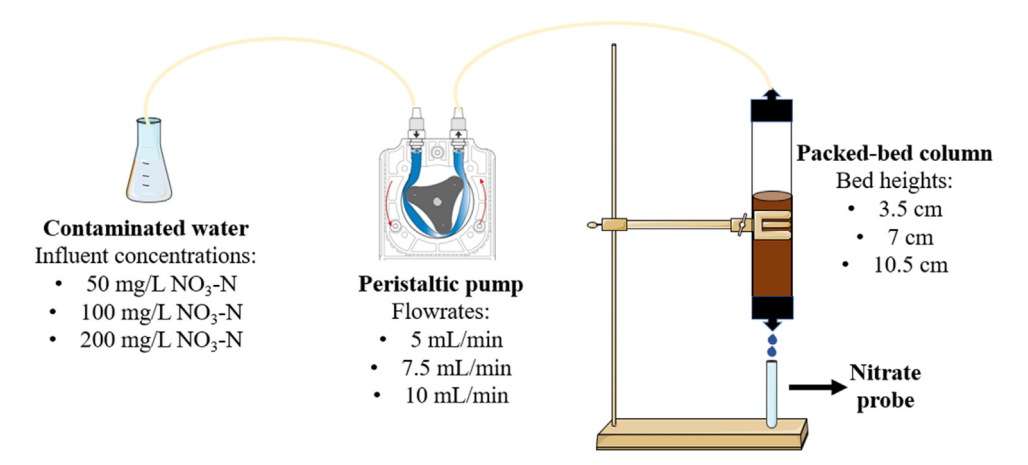


Fig. 1. Schematic representation of experimental setup composed of contaminated water container, peristaltic pump, packed-bed column, and fraction collector to collect column effluent and measure nitrate concentration.

Table 1Parameters of the breakthrough models.

Model	Parameters	Logistic function parameter (a)	Logistic function parameter (b)
Thomas	K_{Th} , q_m	$\frac{K_{Th}q_mM}{O}$	$K_{Th}C_0$
Bohart-Adams	K_{B-A} , N_m	$\frac{Q}{K_{B-A}N_mH}$	$K_{B-A}C_0$
Yoon-Nelson	K_{Y-N} , τ	$K_{Y-N}\tau$	K_{Y-N}

 K_{Th} (L/mg.min) is the Thomas rate constant, q_m (mg/g) is the model adsorption capacity per unit mass of CS-PEI-GLA, $K_{B\text{-}A}$ (L/mg.min) is the Bohart-Adams rate constant, N_m (mg/L) is the model adsorption capacity per unit volume of the bed, H is the height of the bed (cm), u (cm/min) is the linear velocity, $K_{Y\text{-}N}$ (1/min) is the Yoon-Nelson rate constant, and τ (min) is the time when the adsorbate reaches half of the breakthrough.

different amounts of adsorbent (0.25, 0.5 and 0.75 g corresponding to 3.5, 7.0 and 10.5 cm, respectively) while using constant flow rate (5 mL/min) and nitrate concentration (100 mg/mL NO_3^--N) were used to investigate the effect of bed height. The nitrate concentration was analyzed using a nitrate ion-selective electrode (ISE, Thermo Fisher).

2.3. Modeling of the column data

As clearly demonstrated recently in the literature (Hu et al., 2019; Chu, 2020), the three common breakthrough models for modeling adsorption in fix-bed columns in environmental studies namely Thomas, Bohart-Adams, and Yoon-Nelson have similar mathematical forms. Therefore, in this study, the standard logistic function (Eq. 4) was used for fitting of the experimental data and then the three models' parameters were calculated based on Table 1 to elaborate the behavior of the CS-PEI-GLA as packing material for the removal of nitrate,

$$\frac{C_e}{C_0} = \frac{1}{1 + \exp(a - bt)} \tag{4}$$

where a (dimensionless) and b (1/min) are the logistic function parameters that are determined by fitting the experimental data.

Based on assumptions including no resistance to external mass transfer and intraparticle diffusion, the bed depth service time (BDST) model correlates the height of a fix-bed column to the duration that the adsorption system can provide clean water before the concentration in the effluent reaches the maximum safe level (breakthrough point) (Salman Tabrizi and Yavari, 2020; Golie and Upadhyayula, 2016). Eq. 5 shows the BDST model.

$$t_b = \frac{N_{BDST}H}{C_0 u} - \frac{1}{K_{BDST}C_0} \ln(\frac{C_0}{C_b} - 1)$$
 (5)

where N_{BDST} is the model volumetric adsorption capacity (mg/L), K_{BDST} is the model rate constant (L/mg.min), and C_b (mg/L) is the nitrate concentration at outlet of the column at the breakthrough point, which for nitrate was 10 mg/L NO_3^- -N. By plotting the breakthrough time at different bed heights, the model's constants can be calculated.

2.4. Effect of coexisting ions on nitrate removal

A mass of 0.5 g of CS-PEI-GLA was swollen in deionized water and packed in the column in a similar manner as described in section 2.2. The effect of chloride and sulfate on nitrate adsorption in the column was investigated with three different solutions. namely: influent containing nitrate (100 mg/L NO₃ -- N) spiked with 10 times chloride concentration (1000 mg/L Cl⁻) by adding NaCl (1648 mg/L), influent containing nitrate (100 mg/L NO₃⁻-N) spiked with 10 times sulfate concentration (1000 mg/L SO₄²⁻) by adding Na₂SO₄ (1480 mg/L), and influent containing 100 mg/L of nitrate-N and 1000 mg/L of chloride and sulfate, respectively. Solution with only 100 mg/L of nitrate-N was used as control. A flow rate of 5 mL/min was selected for these sets of experiments. Effluents were collected in 20 min intervals and analyzed using ISE. These concentrations of sulfate and chloride were chosen since their concentrations in surface water can be as high as 1000 mg/L (Samadder et al., 2017; Khan et al., 2020).

2.5. Recovery of nitrate and regeneration of the column

The column was loaded with nitrate by introducing 100 mg/L NO_3^- -N solution until the saturation point of the breakthrough curve was achieved (plateau in the curve). Then regenerant solutions, 0.1 M NaOH, 0.1 M HCl, 0.1 M NaHCO $_3$, 0.8 M CH $_3$ COOH, and 0.5 M NaCl were introduced to the saturated column at 5 mL/min. Samples were collected every minute and the nitrate concentrations were analyzed until the nitrate concentration in the effluent reached zero. After regeneration of the column, deionized water was used to remove the residual regenerant in the column and prepare it for the next adsorption cycle. The best regenerant was used ten times for the adsorption/desorption process.

2.6. Nitrate removal from a real water sample

The performance of the column in a real water chemistry to remove nitrate was investigated. The column was prepared as described in section 2.2. The drinking water sample was obtained from the community water services (CWS), Oklahoma City, OK,

with a nitrate concentration of 1.5 times higher than the WHO standard. The water was analyzed for nitrate, phosphate, and total organic carbon (TOC) concentrations and then introduced to the column at 5 mL/min flow rate. Effluent samples were collected every 100 s and analyzed for the same substances. Nitrate concentration was measured by ISE as described before. Phosphate and TOC concentrations were measured using the ascorbic acid method (Maher and Woo, 1998) and potassium hydrogen phthalate (KHP), respectively. For the Total Organic Carbon, we used the TOC Analyzer (Shimadzu).

3. Results and discussion

3.1. Synthesis and characterization of CS-PEI-GLA

To avoid precipitation of CS in the presence of the concentrated PEI solution caused by the high pH value of the mixture, the PEI was dissolved in HCl (25 %) before mixing with the chitosan solution. The resulting mixture had a pH of around 5.5–6.0 and allowed CS to get mixed efficiently with PEI. The use of glutaraldehyde as a crosslinking agent provided an easy method to render the mixture into an insoluble gel form. The optimization and characterization of the adsorbent can be found in our previous publication (Nadres et al., 2017a).

In summary, the adsorbent with 2%, 10 %, and 2% of CS, PEI, and GLA, respectively, had the highest adsorption capacity, therefore, this composition was used in the current study. ATR-FTIR spectra (Fig. S1) showed the characteristic peaks belong to both CS and PEI in CS-PEI-GLA, including -N-H and -O-H stretching vibration, -N-H bending, and -C-N and C—O—C stretching, as well as the stretching of -C-H in PEI (Nadres et al., 2017b; Nie et al., 2005). In the XPS analysis (Table S1), higher nitrogen content was detected in CS-PEI-GLA compared to CS due to the presence of nitrogen-rich PEI. Amine and imine functional groups were detected in CS-PEI-GLA by peak deconvolution (Fig. S2). SEM image (Fig. S3) showed a porous material with creases and grooves. This structure provided a high specific surface area, which was determined to be 462 m²/g with 32.1 Å pore width by BET (Nadres et al., 2017b; Ouyang and Liang, 2014).

3.2. Nitrate adsorption optimization: column experiments

The breakthrough curve was obtained by plotting C_e/C_0 of the nitrate removed by the column against time. This plot allowed the evaluation of the removal of nitrate using the column packed with CS-PEI-GLA. The region of the curve that shows the sudden increase in the concentration of nitrate is called the mass-transfer zone (MTZ) or the adsorption region. This zone shows that the column reaches equilibrium quickly and data from this region can be used in the model fitting (Chu, 2020). In some of the breakthrough curves, the later part of the curves $(C_e/C_0>0.6)$ exhibits intraparticle diffusion, which is the region when the shape of the curve changes direction. This behavior is unaccounted for the model used. Therefore, only the earlier points in the adsorption region were computed to determine more relevant constants for the column characteristics (Li et al., 2020). The important factors that affect an adsorption column performance are flow rate, pollutant concentration, and bed (column) height. The correlation between these parameters and nitrate adsorption was investigated as described below:

3.2.1. Effect of flow rate

Flow rate is one of the most important factors that determines a packed column performance to remove contaminants from the aqueous phase, as it affects the flow residence time in the column (Xu et al., 2013; Nur et al., 2015). Fig. S4 (a) and Table 2 show how

flow rate can change the breakthrough curve and column parameters, respectively. Fig. S4 (a) shows that the breakthrough curve has shifted to the left and resulted in a shorter $t_{\rm b}$, at higher flow rates (Table 2). By increasing the flow rate, the column reached its breakthrough point faster and the adsorption capacity ($q_{\rm exp}$), percent removal (R), and the total volume of water up to the breakthrough point ($V_{\rm b}$) (Table 2) decreased, which means a lower volume of clean water can be achieved by increasing the flow rate.

By fitting the experimental data to a logistic function, the model parameters for Bohart-Adams, Thomas, and Yoon-Nelson models were calculated and presented in Table 3. The data showed good agreement with the logistic function as the regression coefficient (R^2) was bigger than 0.96 in all the three conditions. The models' kinetic constants ($K_{B-A},\,K_{Th},\,$ and K_{Y-N}) increased with increasing in flow rate, while adsorption capacity (q_m and N_m), as well as $\tau,$ decreased when flow rate increased. Furthermore, the experimental adsorption capacity (q_{exp}) and the Thomas model adsorption capacity (q_m) were close, with less than 5% difference, which further proves the model describes well the lab-scale fix-bed column.

Changing the flow rate can have various effects on the continuous adsorption process. On one hand, the increase in flow rate could be detrimental to adsorption since adsorbate and the adsorbent will be in contact for a shorter period of time, which may prevent the adsorption process to reach equilibrium (Salman Tabrizi and Yavari, 2020; Xu et al., 2013; Wu et al., 2016; Olgun et al., 2013; Golie and Upadhyayula, 2016). This effect can be observed at 7.5 and 10 mL/min flow rates, where the column reached the breakthrough points earlier and the adsorption capacity and percent removal were lower compared to the 5 mL/min. On the other hand, if external mass transfer resistance controls the adsorption rate, an increase in the turbulence of the flow by increasing the flow rate must provide lower external resistance and increase in rate constants (Salman Tabrizi and Yavari, 2020; Najmi et al., 2020; Xu et al., 2013; Wu et al., 2016; Jana et al., 2020; Xu et al., 2018). Therefore, the fact that, rate constants increased when flow rate increased, indicates that external mass transfer resistance is dominant (Xu et al., 2013; Li et al., 2020; Zhang et al., 2016). It should be noted that, although an increase in flow rate decreased the volume of the clean water that could be obtained, this amount of clean water was produced in a shorter time.

3.2.2. Effect of concentration

Pollutant concentration can affect different aspects of the adsorption process. Investigating the effect of three concentrations of nitrate-N (50, 100, and 200 mg/L) at a fixed flow rate (5 mL/min) on the breakthrough behavior of the column showed that the curve moved to left and breakthrough time shortened when the influent concentration increased (Fig. S4 (b) & Table 2). V_b and R were higher at low concentrations, while q_{exp} increased when the influent concentration increased (Table 2). Like the effect of flow rate experiments, the logistic function fitted well with the experimental data with R^2 higher than 0.96 at all conditions (Table 3). While K_{Y-N} showed a direct relationship with nitrate concentration, K_{B-A} , K_{Th} , q_m , N_m , and τ were negatively related to nitrate concentration.

A change in concentration had an impact on the mass transfer of the solutes into the adsorbent (Goel et al., 2005). By increasing the solute concentration, the mass transfer driving force increased, therefore, adsorption capacity increased, and more solutes attached to the adsorbents' binding sites leading to shorter breakthrough time and τ (Salman Tabrizi and Yavari, 2020; Olgun et al., 2013; Golie and Upadhyayula, 2016). However, the adsorption process became less kinetically favorable as K_{B-A} and K_{Th} decreased (Li et al., 2020; Zhang et al., 2016). On the other hand, at higher concentrations, the amount of ions not adsorbed to the adsorbent increased, which led to lower percent removal (Salman Tabrizi and Yavari, 2020; Najmi et al., 2020; Zhong et al., 1997). The

Table 2 Parameters of column experiments.

Run #	Q (mL/min)	C ₀ (mg/L)	H (cm)	M (g)	t _b (min)	q _{exp} (mg/g)	R (%)	V _b (mL)
1	5	100	7	0.5	85	121.56	79.06	425
2	7.5	100	7	0.5	52	121.16	77.27	390
3	10	100	7	0.5	38	116.50	70.35	380
4	5	50	7	0.5	180	100.32	86.73	900
5	5	200	7	0.5	52	159.06	66.55	260
6	5	100	3.5	0.25	30	76.12	54.26	150
7	5	100	7	0.5	70	88.66	59.54	350
8	5	100	10.5	0.75	115	92.61	61.91	575

Q(mL/min) is the flow rate, $C_0(mg/L)$ is the nitrate-N concentration in influent, H(cm) is the bed height, M(g) is the adsorbent mass, $t_b(min)$ is the breakthrough time, $q_{exp}(mg/g)$ is the experimental adsorption capacity, R(%) is nitrate removal, and $V_b(mL)$ is the effluent volume up to the breakthrough point.

Table 3Parameters for the Bohart-Adams, Thomas, and Yoon-Nelson models.

Run #	R ²	K _{BA} , K _{Th} * 10 ⁻⁴ (L/mg.min)	N _m (mg/L)	q _m (mg/g)	K _{YN} * 10 ⁻² (1/min)	τ(min)
1	0.9639	10.51	5106.56	126.27	12.93	102.66
2	0.9592	12.25	4767.00	117.88	13.70	70.28
3	0.9614	15.56	4483.14	110.86	16.10	53.55
4	0.977	11.98	4128.26	102.08	5.50	222.4
5	0.9817	6.57	5565.27	137.62	12.56	71.97
6	0.9102	7.19	2971.59	73.48	7.20	36.67
7	0.9626	7.71	3782.99	93.54	7.97	90.47
8	0.9558	9.06	3893.58	96.28	9.37	139.67

 R^2 is the regression coefficient, K_{Th} (L/mg.min) is the Thomas rate constant, q_m (mg/g) is the model adsorption capacity per unit mass of CS-PEI-GLA, K_{B-A} (L/mg.min) is the Bohart-Adams rate constant, N_m (mg/L) is the model adsorption capacity per unit volume of the bed, K_{Y-N} (1/min) is the Yoon-Nelson rate constant, and τ (min) is the time when adsorbate reaches half of the breakthrough.

adsorption capacity, q_{exp} and q_m , values were close (Table 2 & 3), which further highlights the models describe well the adsorption system.

3.2.3. Effect of bed height

Different amounts of packing materials can be used in a column, which can affect the column behavior. In this set of experiments, it was observed that a bigger amount of the adsorbent (higher bed height) resulted in longer breakthrough time and a larger volume of clean water (Fig. S4 (c) & Table 2). Moreover, the adsorption capacity, percent removal increased, models' kinetic constants, and τ from the Yoon-Nelson model increased with higher bed heights (Table 2 & 3). The calculated adsorption capacity from the Thomas model was in the 5% range of q_{exp} for all the bed heights investigated (Table 3)

Bed height can alter two important factors in a continuous adsorption system, namely the number of adsorption sites and the time that solution spends in the column (flow residence time). Higher bed height provides more adsorption sites for nitrate ions, as a result, the breakthrough time and volume of the clean water increased by increasing the bed height from 3.5 cm to 10.5 cm (Salman Tabrizi and Yavari, 2020; Olgun et al., 2013; Golie and Upadhyayula, 2016). Moreover, when the bed height increased, the pollutants spent more time in the column in contact with the adsorbents, therefore, the adsorption process got closer to equilibrium (Salman Tabrizi and Yavari, 2020; Wu et al., 2016; Olgun et al., 2013; Golie and Upadhyayula, 2016). This effect could be observed by the increasing percent removal and adsorption capacity of the CS-PEI-GLA when the column height increased (Zhong et al., 1997). Higher kinetic constants at higher bed heights, demonstrated that axial dispersion did not increase due to increase in the bed height. Therefore, the flow type was close to the plug flow, which agreed with the Thomas model assumption. (Li et al., 2020).

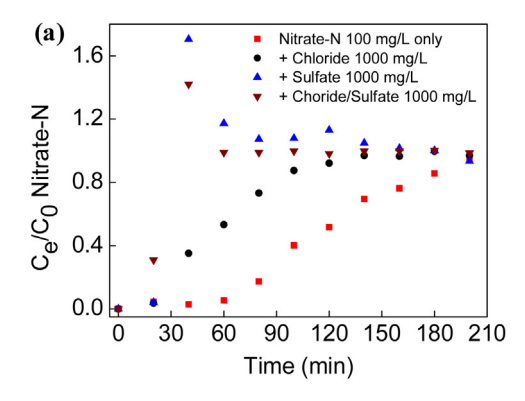
BDST model was fitted to the experimental t_b vs. H data (Fig. S4 (d)). The R^2 was 0.9977 and the model's parameters determined to be N_{BDST} = 3554.38 (mg/L) and K_{BDST} = 0.0014 (L/mg.min). This model can be used for scale-up purposes. By having the model's parameters and desired operational conditions, the service time of

the column can be calculated, which is essential for proper maintenance of the adsorption system (Golie and Upadhyayula, 2016).

3.3. Effect of coexisting ions on nitrate removal

Chloride and sulfate are among the most common anions that can be found in surface water and groundwater. Therefore, for a real application, it is important to study how these coexisting anions affect nitrate adsorption on CS-PEI-GLA. The presence of chloride, sulfate, and chloride/sulfate affected differently the breakthrough curves and CS-PEI-GLA adsorption capacities for nitrate (Fig. 2). When the column packed with CS-PEI-GLA was injected with only nitrate, the breakthrough time was around 50 min. The presence of 1000 mg/L of chloride significantly lowered the breakthrough time to around 20 min. Clearly, the chloride ions influence the interaction between the nitrate and the CS-PEI-GLA adsorbent. The existence of 1000 mg/L sulfate shifted the breakthrough time of nitrate similarly to chloride. When both chloride and sulfate were added to the influent, the t_b decreased to around 5 min. Normalized nitrate concentration increased gradually in the solution spiked only with chloride and resulted in the typical Sshaped breakthrough curve. However, for samples with sulfate, the breakthrough curves had a significantly different shape. For these samples, after the breakthrough time, the concentration of nitrate had become greater than the influent concentration for a while, then the normalized concentration reached a plateau at a value of 1 (Fig. 2 (a)). Calculating the adsorption capacity in different conditions showed that, chloride decreased the adsorption capacity for nitrate to around half, while almost no nitrate remained attached to the adsorbent in the column in the presence of sulfate at 1000 mg/L (Fig. 2 (b)).

Chloride negatively affected nitrate removal by occupying some adsorption sites, however, the adsorption system was still able to adsorb a portion of nitrate ions in the presence of chloride, while for sulfate this effect was more adverse as almost all the adsorption sites were filled with sulfate ions instead of nitrate. The same trend was observed by Wu et al. (Wu et al., 2016) when they used an amine modified polymeric adsorbent to remove nitrate in the



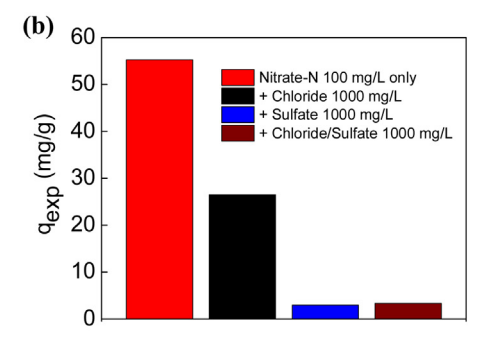


Fig. 2. Effect of excess chloride and sulfate on the nitrate removal by 0.5 g of CS-PEI-GLA from solutions containing: (i) 100 mg/L of Nitrate-N, (ii) 100 mg/L of Nitrate-N + 1000 mg/L of Coloride, (iii) 100 mg/L of Nitrate-N + 1000 mg/L of Sulfate, and (iv) 100 mg/L of Nitrate-N + 1000 mg/L of Coloride + 1000 mg/L of Sulfate: (a) nitrate breakthrough curve and (b) q_{exp}.

presence of chloride and sulfate. An unusual spike in nitrate concentration between 20-60 min of the adsorption process (C_e/C_0 > 1) could be justified by the fact that some nitrate ions initially adsorbed to the CS-PEI-GLA in the first 20 min and later were replaced by sulfate ions, which resulted in higher effluent concentration for nitrate than in the influent. The effect of chloride and sulfate on the column performance can be explained by three reasons: 1) The main adsorption sites on the adsorbent are amine and hydroxyl groups (Nadres et al., 2017a). While chloride can only attach to amine groups by coulombic interaction, oxyanions like sulfate can form strong hydrogen bonds with amine and hydroxyl functional groups on CS-PEI-GLA on top of coulombic interaction (Salman Tabrizi and Yavari, 2020; Wu et al., 2016). Therefore, in the presence of excess chloride not all the adsorption sites were occupied, and nitrate removal was observed to a certain amount. However, sulfate competes with nitrate for both adsorption sites and is more likely to attach to the amine and hydroxyl groups as explained below. 2) The origin of selectivity arises from the configuration of the adsorption sites, specifically to the distance between two positively charged cationic sites. More isolated cationic sites tend to favor nitrate adsorption. As the proximity of the cationic sites becomes smaller, enough to be bridged by divalent sulfate ions, adsorption favors the latter (Jackson and Bolto, 1990). 3) Basic functional groups like amine groups have selectivity toward divalent ions (Dominguez et al., 2003). The adsorption system did not show a good performance in the presence of high concentrations of chloride and sulfate. However, it should be noted that we investigated the worst-case scenario and the performance of the adsorbent might be better when lower concentrations of chloride or sulfate are present.

3.4. Recovery of nitrate and regeneration of the column

The life cycle of the column would be extremely attractive if it could be recycled. In addition, the recovery of the nitrates that were bound in the column could provide an opportunity for recycling the nutrient to be used as fertilizers (Hube et al., 2020). Experiments were done to determine the best agent for the recovery of the nitrate and to result in a column ready for another round of nitrate removal.

3.4.1. Recovery of nitrate using different reagents

Investigating the performance of different reagents to desorb nitrate from CS-PEI-GLA gives insights on the mechanism operating in the nitrate recovery process. The percentage of nitrate recovered from the column with hydrochloric acid 0.1 M, a strong acid, sodium hydroxide 0.1 M, a strong base, sodium bicarbonate 0.1 M, a weak base, acetic acid 0.8 M, a weak acid, and sodium chloride 0.5 M is

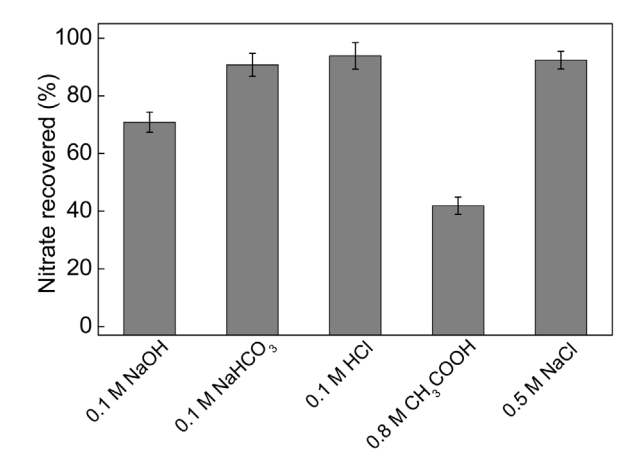


Fig. 3. Recovery of nitrate from saturated columns ($0.5 \, g$ of CS-PEI-GLA) by different reagents. Columns were saturated by $100 \, mg/L \, NO_3$ -N at $5 \, mL/min$. The reagents introduced to the column at $5 \, mL/min$ until no nitrate was detected in the effluent.

demonstrated in Fig. 3. Acetic acid had the worst recovery, followed by sodium hydroxide, while the percentage of nitrate recovered with sodium bicarbonate, hydrochloric acid, and sodium chloride was above 90 %.

Based on Fig. 3 one of the best reagents to recover the nitrate was NaHCO₃, recovering 90.8 \pm 4 % nitrate from the column. In addition to good recovery, presence of sodium bicarbonate in the nitrate-rich water collected from the column after recovery, can provide an excellent fertilizer with fungicidal property (Zamani et al., 2007). The most plausible mechanism that explains why NaHCO₃ is efficient in recovery is that the basic nature of NaHCO₃ solution deprotonates the ammonium groups of CS-PEI-GLA. The deprotonation could result in uncharged amine groups, weakening the electrostatic bond with the nitrate ions, releasing these ions (Jóźwiak et al., 2014; Nadres et al., 2017b). Moderately efficient regeneration (70.9 \pm 3.5 % recovery) was also observed when NaOH solution was used as a recovery agent. A solution of NaOH is highly basic, which can also favor the deprotonation of ammonium groups and successive release of the held nitrate ions, however, compression of the polymer composite adsorbent in the column was observed when NaOH was used as a regenerant. This change in the CS-PEI-GLA material might have affected its porosity, which can explain the lower nitrate recovery when NaOH was used compared to NaHCO₃ (Jóźwiak et al., 2014). While NaHCO₃ was very good in recovering nitrate, the amine groups resulted from the recovery became unprotonated, hence could no longer form electrostatic interactions with the nitrate in the column. As a result, when another batch of nitrate solution was added to the column

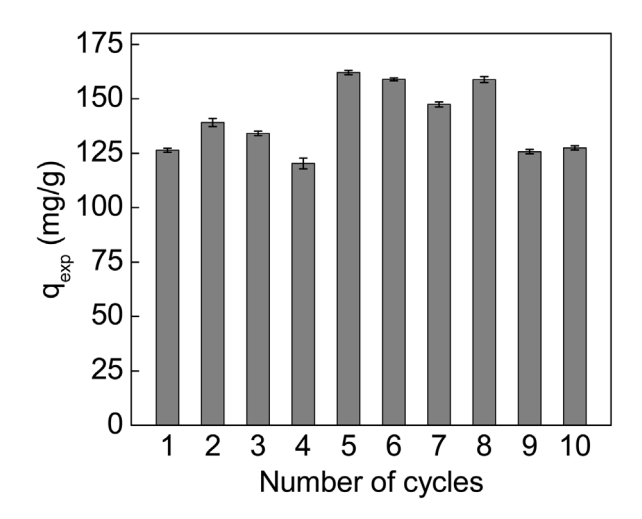


Fig. 4. The adsorption capacity of the columns packed with 0.5 g of CS-PEI-GLA adsorbent for nitrate removal after regeneration with NaCl 0.5 M for ten cycles. Columns were saturated by 100 mg/L NO_3 -N at 5 mL/min. The reagent introduced to the column at 5 mL/min until no nitrate was detected in the effluent.

after recovery, the nitrate removal efficiency became very low. This loss of nitrate removal activity was also observed when NaOH was used as a recovery agent. For recovery agent such as sodium bicarbonate, although the nitrate recovery was high, the column was left unusable for another round of nitrate adsorption.

Meanwhile, the use of HCl solution was proved to be effective in recovering the column (93.9 \pm 4.6 % recovered). The recovery of nitrate using acidic substances such as HCl undergoes different mechanisms compared to the basic regenerants. Under acidic conditions, the amine group is constantly protonated. However, chloride ions (from HCl) can replace the nitrate on the adsorption sites, hence nitrates can be recovered. For acetic acid, the weak acetate ions were not preferred compared to nitrate, as a result, low recovery was obtained (41.9 \pm 3 %) (Xu et al., 2013).

On the other hand, the sodium chloride was also efficient in removing nitrate bound to the CS-PEI-GLA, recovering $92.4\pm3.1\,\%$ of nitrate from the column. The presence of excess chloride ions displaced the nitrate ions held by electrostatic attraction in the adsorption sites. In this mechanism, the ammonium adsorption sites were positively charged (Jóźwiak et al., 2014; Xing et al., 2011; Nadres et al., 2017b). Sodium chloride solution effectively regenerated the column and allowed it to be ready for another round of nitrate adsorption. Therefore, sodium chloride was preferred to hydrochloric acid since it caused less environmental hazards and was easier to work with. Besides, the recovered water could also be potentially used as a fertilizer for marine algae growth.

3.4.2. Regeneration cycles

Fig. 4 shows the adsorption capacity of the column after each adsorption/desorption. For ten adsorption/desorption cycle the q_{exp} was in the 125–160 mg/g range. In some cycles, adsorption and regeneration resulted in higher adsorption capacity compared to the fresh column, probably due to opening of sites that were not previously available. As explained in section 3.4, chloride ions can compete with nitrate ions for adsorption sites. However, in that section, it was observed that some nitrate ions still remained attached to the adsorbent in the presence of chloride. In the recovery experiments, since the chloride concentration was about 18 times higher than chloride concentration in section 3.4, it is reasonable to assume that all the adsorbed nitrate ions were replaced by chloride ions due to high mass transfer driving force for chloride. But when a fresh nitrate solution was introduced to the column after desorption, nitrate ions were able to occupy the adsorption

Table 4Characteristics of the CWS water sample (adapted from Nadres et al. (2017a)).

Parameters	Initial value	
pН	7.0	
TOC	35.0 ± 0.4 mg/L	
Nitrate-N	15.4 ± 0.9 mg/L	
Phosphate	$2.37\pm1.5~mg/L$	

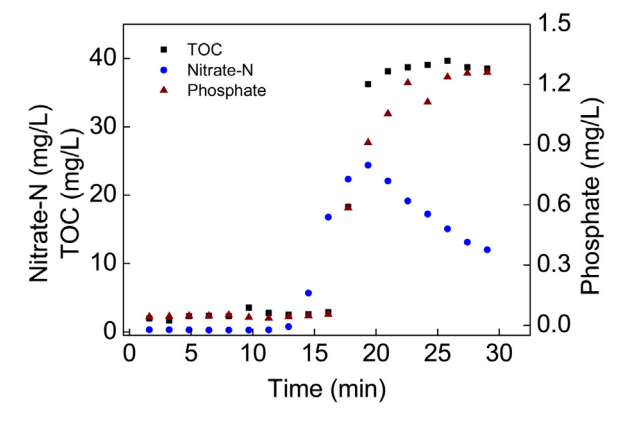


Fig. 5. Breakthrough curve for nitrate removal from the real water system at 5 mL/min by column packed with 0.5 g of CS-PEI-GLA. In addition to nitrate, contaminants such as phosphate and total organic carbon were removed.

sites and detach chloride. After ten cycles, the adsorption capacity did not change much from the initial value. This result has a large implication on the utility of the CS-PEI-GLA in repeated use. Nitrate-rich saltwater collected from the column regeneration can have potential use as a fertilizer in saltwater algae cultures, that is used for biofuel production (Hannon et al., 2010; Khan et al., 2018).

3.5. Nitrate removal from a real water sample

The polymer composite absorbent was further tested for use in drinking water. As shown in Table 4, the nitrate concentration of the selected groundwater was about 1.5 times higher than that of the WHO safety level.

According to Fig. 5, in addition to nitrate, other contaminants such as the negatively charged phosphate and TOC were removed from the water by the polymer composite adsorbent. The mechanism of removal was presumably the active ammonium sites, which formed a strong electrostatic bond with phosphate and organic carbons. The organic carbons mainly contained negatively charged humic and fulvic acids, due to opposing charges. It can be observed that after around 16 min, some previously adsorbed nitrate ions were replaced by either phosphate or TOC, which resulted in increasing nitrate concentration in the effluent than the influent. This shows that the adsorption sites are not specific to nitrate, as observed in section 3.4. After around 30 min, the column reached equilibrium as the nitrate concentration in the influent and the effluent were the same. The fact that TOC concentration did not exceed the influent value signifies that the adsorbent is stable, and it is not leaching its components to the water. This experiment showed that CS-PEI-GLA can effectively remove different contaminants in the complex chemistry of a real water sample.

4. Conclusion

A stable amine-rich polymer composite containing CS and PEI crosslinked with GLA was prepared and used in continuous mode in a packed bed column to adsorb nitrate from water. The effect of different operational parameters on the breakthrough curve and column performance was investigated. The breakthrough models'

constants were calculated, and it was determined that the models' rate constant increased with flow rate, indicating external mass transfer determines the adsorption kinetics. The higher adsorption capacity of the column was achieved at a low flow rate, high influent concentration, and high bed height. The adsorbent was determined to be not selective towards nitrate only, as a high concentration of chloride decreased nitrate removal, and a high concentration of sulfate almost completely prevented nitrate adsorption to CS-PEI-GLA. However, facile regeneration of the column with NaCl for 10 adsorption/desorption cycles without loss of adsorption capacity was achieved. It should be highlighted that the recovered nitrate in the salt solution can be used as an algae fertilizer. Therefore, in this study, nitrate was transformed from a pollutant to a valuable component. Lastly, by investigating real water samples, we demonstrated that the adsorption system was effective in removing nitrate, phosphate, and TOC, which makes CS-PEI-GLA a good candidate for practical applications in water treatment.

Declaration of Competing Interest

The authors declare that they have no known competing financial interests or personal relationships that could have appeared to influence the work reported in this paper.

Acknowledgments

This work was partially supported by the US Department of Interior, Bureau of Reclamation through the Desalination and Water Purification Research and Development Program (Agreement No. R16AC00123); the Welch foundation award number (E-2011-20190330); and the National Science Foundation under Grant No. CHE-1904472.

Appendix A. Supplementary data

Supplementary material related to this article can be found, in the online version, at doi:https://doi.org/10.1016/j.psep.2021.04.027.

References

Berbar, Y., Amara, M., Kerdjoudj, H., 2012. Procedia Eng. 33, 126-133.

```
Chu, K.H., 2020. Chem. Eng. J. 380, 122513.
Crini, G., Badot, P.-M., 2008. Prog. Polym. Sci. 33, 399-447.
Dominguez, L., Economy, J., Benak, K., Mangun, C.L., 2003. Polym. Adv. Technol. 14,
Dutta, P.K., Dutta, J., Tripathi, V.S., 2004. J. Sci. Ind. Res. (India) 63, 20-31.
Goel, J., Kadirvelu, K., Rajagopal, C., Kumar Garg, V., 2005. J. Hazard. Mater. 125,
    211 - 220
Golie, W.M., Upadhyayula, S., 2016. J. Water Process. Eng. 12, 58-65.
Hannon, M., Gimpel, J., Tran, M., Rasala, B., Mayfield, S., 2010. Biofuels 1, 763-784.
Hu, Q., Xie, Y., Feng, C., Zhang, Z., 2019. Chem. Eng. J. 358, 1471-1478
Hube, S., Eskafi, M., Hrafnkelsdóttir, K.F., Bjarnadóttir, B., Bjarnadóttir, M.Á., Axels-
    dóttir, S., Wu, B., 2020. Sci. Total Environ. 710, 136375
Jackson, M.B., Bolto, B.A., 1990. React. Polym. 12, 277-290.
Jana, A., Roy, O., Ravuru, S.S., De, S., 2020. Chem. Eng. J. 391, 123587.
Jóźwiak, T., Filipkowska, U., Szymczyk, P., Mielcarek, A., 2014. PCACID 19, 41-52.
Khan, M.I., Shin, J.H., Kim, J.D., 2018. Microb. Cell Fact. 17, 36-36.
Khan, M.R., Wabaidur, S.M., Busquets, R., AlAmmari, A.M., Azam, M., Alsubhi, A.,
    2020. J. King Saud Univ. - Sci. 32, 1986-1992
Li, Y., Liu, S., Wang, C., Ying, Z., Huo, M., Yang, W., 2020. J. Hazard. Mater. 386, 121942.
Maher, W., Woo, L., 1998. Anal. Chim. Acta 375, 5-47
Medina, R.P., Nadres, E.T., Ballesteros, F.C., Rodrigues, D.F., 2016. Environ. Sci. Nano
Nadres, E.T., Perez, J.V.D., Rodrigues, D.F., 2017a. Proc. Water Environ. Fed., 438-460.
Nadres, E.T., Perez, J.V.D., Rodrigues, D.F., 2017b. Proc. Water Environ. Fed., 438-460.
Najmi, S., Hatamipour, M.S., Sadeh, P., Najafipour, I., Mehranfar, F., 2020. SN Appl.
Nie, B., Stutzman, J., Xie, A., 2005. Biophys. J. 88, 2833-2847.
Nur, T., Shim, W.G., Loganathan, P., Vigneswaran, S., Kandasamy, J., 2015. Int. J.
    Environ. Sci. Technol. 12, 1311-1320.
Olgun, A., Atar, N., Wang, S., 2013. Chem. Eng. J. 222, 108-119.
Ouyang, A., Liang, J., 2014. RSC Adv. 4, 25835-25842.
Perez, J.V.D., Nadres, E.T., Nguyen, H.N., Dalida, M.L.P., Rodrigues, D.F., 2017. RSC Adv.
    7, 18480–18490.
Rao, X., Tatoulian, M., Guyon, C., Ognier, S., Chu, C., Abou Hassan, A., 2019. Nanoma-
    terials Basel (Basel) 9, 1034
Salman Tabrizi, N., Yavari, M., 2020. J. Environ. Sci. Health A 55, 777-787.
Samadder, S.R., Prabhakar, R., Khan, D., Kishan, D., Chauhan, M.S., 2017. Sci. Total
    Environ. 580, 593-601.
Sun, Y., Zheng, W., 2020. Chemosphere 258, 127373.
Wu, Y., Wang, Y., Wang, J., Xu, S., Yu, L., Philippe, C., Wintgens, T., 2016. J. Taiwan
    Inst. Chem. Eng. 66, 191-199.
Xing, X., Gao, B.-Y., Zhong, Q.-Q., Yue, Q.-Y., Li, Q., 2011. J. Hazard. Mater. 186,
    206-211
Xu, X., Gao, B., Tan, X., Zhang, X., Yue, Q., Wang, Y., Li, Q., 2013. Chem. Eng. J. 226,
```

Xu, L., Wang, S., Zhou, J., Deng, H., Frost, R.L., 2018. Chem. Eng. J. 335, 450–457. Zamani, M., Sharifi Tehrani, A., Ali Abadi, A.A., 2007. Commun. Agric. Appl. Biol. Sci.

Zhong, G., Sajonz, P., Guiochon, G., 1997. Ind. Eng. Chem. Res. 36, 506–509.

Zhang, X., Bai, B., Li Puma, G., Wang, H., Suo, Y., 2016. Chem. Eng. J. 284, 698-707.